Journal of Simulation & Analysis of Novel Technologies in Mechanical Engineering
10 (2) (2017) 0021~0034
HTTP://JSME.IAUKHSH.AC.IR
ISSN: 2008-4927

Stirred Tank Fluid Flow Simulation with Two Lattice Boltzmann Methods

Seyyed Mehdi Naghavi*

Department of Mechanical Engoneerinh, Khomeinishahr Branch, Islamic Azad University, Isfahan, 84175-119, Iran.

**Corresponding Author: Naghavi@iaukhsh.ac.ir*

(Manuscript Received --- 04, 2017; Revised --- 06, 2017; Accepted --- 07, 2017; Online --- 09, 2017)

Abstract

In the present study, commonly used weakly compressible lattice Boltzmann method and Guo incompressible lattice Boltzmann method have been used to simulate fluid flow in a stirred tank. For this purpose a 3D Parallel code has been developed in the framework of the lattice Boltzmann method. This program has been used for simulation of flow at different geometries such as 2D channel flow and 3D stirred tank flow. It has been shown that in addition to elimination of compressibility error, the Guo incompressible method eliminates mass leakage error from the fluid flow simulations although its implementation is as easy as the weakly compressible Lattice Boltzmann method. For example in presented stirred tank problem mass leakage in Guo method is about 0% while for LBGK method is about 1.4%. By the way, comparison between results of the two methods shows that differences in local flow quantities are negligible in both methods; however, for overall flow quantities, the results of Guo incompressible method are more accurate than those of weakly compressible method.

Keywords: Lattice Boltzmann method; Stirred tank; Turbulent flow; Guo Incompressible lattice Boltzmann method; parallel programming.

1- Introduction

Turbulently agitated stirred tanks are encountered in a large variety of industrial processes. Optimization of mixing in stirred tanks largely depends on a good understanding of their hydrodynamics. Numerical methods, capable of simulating fluid flow in stirred tanks, have been proven very useful in mixing technology. However, for the sake of turbulent flow complexity in stirred tanks and their 3D asymmetry flow, simulation is impossible without some simplifications. Eggels ([1]) was the first to report on large eddy simulation (LES) in a stirred tank configuration using the lattice Boltzmann method (LBM)[2-19]. The snapshots of the flow field, presented in his article, give a very good view of the turbulent flow structures in the vessel. The agreement with experimental data was good. In the article; however, only a comparison with phase-averaged velocity measurement has been made. In that work, fluid flow has been simulated in a stirred tank with four

baffles and a six bladed Rushton turbine. For the sake of asymmetric turbulent flow in the stirred tank, the whole tank has been simulated. For the simulation of incompressible fluid flow in the tank, weakly compressible lattice Boltzmann method has been used. And to eliminate compressibility error from the simulation, conditions have been selected so that Mach number was low enough and compressibility error, which is proportional to Mach number into the power of two, was negligible. Also in this work, moving blades have been removed from the simulation, and their effects have been applied by some force terms which is called force field method in the literatures. Fluid flow in a stirred tank has been simulated by Derksen and Van Den Akker [20] in other work. In their simulation, four baffles and a six bladed Rushton turbine exist in the tank. For simulation of turbulent flow, LES has been used. Similar to previous lattice Boltzmann work, in their work blades have been removed from the domain and their effects have been applied by a force field method. By the way, similar to Eggels work, low Mach number has been used for small compressibility effect. After this work, many works have been done by Derksen and several others by the lattice Boltzmann method for simulation of fluid flow in stirred tanks for example [21-25]. In all of these works, for simulation of incompressible flow, weakly compressible lattice Boltzmann has been used in which compressibility error were negligible due to low Mach number. Major difference between these works are number of baffles, pitched blades or Rushton turbine blades, two phase or single phase simulation, uniform or nonuniform grid application and etc. A computer code, based on the lattice Boltzmann method has been prepared to simulate the turbulent flow in a stirred tank. An eddy viscosity model has been incorporated in the code so that it can do large eddy simulation for highly turbulent flows. As stated in the literature survey, in all works that have been done with the lattice Boltzmann method, for fluid flow simulation in stirred tanks, weakly compressible lattice Boltzmann method has been used with conditions that compressibility error can be neglected. In the present study, an attempt has been made to investigate effects of compressibility error on the fluid flow simulation in a stirred tank. For this purpose, commonly used lattice Boltzmann method and Guo incompressible lattice Boltzmann method [26] are reviewed first, and their differences are shown in one simple problem. After that, fluid flow is investigated in a stirred tank with the two methods.

I. BGK Lattice Boltzmann method

Lattice Boltzmann method is one of the computational fluid dynamic methods for the simulation of fluid flow. In this method, kinetic equation is solved for distribution function, and macroscopic quantities are earned from distribution function in each point [27, 28]. One commonly used kinetic model is Bhatnagar-Gross-Krook (BGK) model. In this model, Boltzmann equation is

$$\frac{\partial f}{\partial t}+\vec{u}\cdot\vec{\nabla}f=-\frac{1}{\lambda}(f-f^{eq}) \quad (1)$$

In which f is distribution function, f^{eq} is equilibrium distribution function (Maxwell-Boltzmann equilibrium distribution function), $\vec{u}$ is fluid particle velocity and λ is relaxation time. In general, one fluid particle can be moved in

infinity directions. The first step to solve Eq. (1), is discretization of fluid particle velocity ($\vec{u}$). For this purpose, fluid particle movements are restricted to special velocities ($\vec{u}_\alpha$) so that conservation laws are not violated

$$\frac{\partial f_\alpha}{\partial t}+\vec{u}_\alpha\cdot\vec{\nabla}f_\alpha=-\frac{1}{\lambda}(f_\alpha-f_\alpha^{eq}) \tag{2}$$

In the above Eq., $f_\alpha\equiv f(\vec{x},\vec{u}_\alpha,t)$ is the distribution function for α'th discretized velocity $\vec{u}_\alpha$, and f_α^{eq} is the corresponding equilibrium distribution function, in the discrete velocity space. Equilibrium distribution function for D3Q19 model, which is one commonly used model in 3D simulations, is defined as

$$f_\alpha^{eq}=\rho w_\alpha[1+\frac{\vec{e}_\alpha\cdot\vec{u}}{C_S^2}+\frac{(\vec{e}_\alpha\cdot\vec{u})^2}{2C_S^4}-\frac{\vec{u}\cdot\vec{u}}{2C_S^2}] \tag{3}$$

In which ρ is fluid density, w_α is weight factor, Eq. (4), $C_S=c/\sqrt{3}$ is speed of sound with $c=\delta x/\delta t$ being the lattice speed, δt being the lattice time step and δx being the lattice length

$$w_\alpha=\begin{cases}1/3 & \alpha=0\\ 1/18 & 1\le\alpha\le6\\ 1/36 & 7\le\alpha\le18\end{cases} \tag{4}$$

And $\vec{e}_\alpha$ denotes the discrete velocity set, as Eq. (5).

$$\vec{e}_\alpha=\begin{cases}(0,0,0) & \alpha=0\\ (\pm1,0,0),(0,\pm1,0),(0,0,\pm1), & 1\le\alpha\le6\\ (\pm1,\pm1,0),(\pm1,0,\pm1),(0,\pm1,\pm1), & 7\le\alpha\le18\end{cases} \tag{5}$$

With this discretization in space and time, distribution function is used for density and momentum computation as

$$\rho=\sum_{\alpha=0}^{18}f_\alpha=\sum_{\alpha=0}^{18}f_\alpha^{eq} \tag{6}$$

$$\rho\vec{u}=\sum_{\alpha=1}^{18}\vec{e}_\alpha f_\alpha=\sum_{\alpha=1}^{18}\vec{e}_\alpha f_\alpha^{eq} \tag{7}$$

Fully discretized form of Eq. (1) with time step δt and space step $\vec{e}_\alpha\delta t$ is as follows:

$$f_\alpha(\vec{x}_i+\vec{e}_\alpha\delta t,t+\delta t)-f_\alpha(\vec{x}_i,t)=-\frac{1}{\tau}[f_\alpha(\vec{x}_i,t)-f_\alpha^{eq}(\vec{x}_i,t)] \tag{8}$$

In which, $\tau=\lambda/\delta t$ is dimensionless relaxation time and $\vec{x}_i$ is coordinate of one point in physical space. This Eq. is called Boltzmann discretized Eq. with BGK approximation (or sometimes LBGK). This Eq. is always solved in two steps as Eqs. (9) and (10). In these Eqs., the distribution function after collision step is shown with ~ sign.

$$\tilde{f}_\alpha(\vec{x}_i,t+\delta t)=f_\alpha(\vec{x}_i,t)-\frac{1}{\tau}[f_\alpha(\vec{x}_i,t)-f_\alpha^{eq}(\vec{x}_i,t)]\ \text{:collision step} \tag{9}$$

$$f_\alpha(\vec{x}_i+\vec{e}_\alpha\delta t,t+\delta t)=\tilde{f}_\alpha(\vec{x}_i,t+\delta t)\ \text{:streaming step} \tag{10}$$

In lattice Boltzmann method, relaxation time τ is computed from kinematic viscosity υ as Eq. (11):

$$\tau=\frac{\upsilon}{C_S^2}+0.5 \tag{11}$$

And pressure from Eq. (12)

$$P=\rho C_s^2 \tag{12}$$

In this method, summation of the distribution function in each point is equal to density in that point, Eq. (6). However, for the sake of streaming step, Eq. (10), this summation is not constant, therefore, density is changed and compressibility error occurs. Small change is occurred in the density value when low Mach number

is used. Due to this small density change the method is called weakly compressible lattice Boltzmann method.

II. Guo Incompressible LBM

To remove compressibility error from the lattice Boltzmann method several methods have been proposed. For example He et al [29] proposed an incompressible lattice Boltzmann method, in which, density is considered as a constant number and pressure is computed from the distribution function. Doing so, density is a constant number and compressibility error is removed from the simulation however, distribution function errors affect the pressure and then affect the flow field. Minimizing compressibility effect another method has been proposed by Dellar [30]. Nevertheless, in end of simulation with that method, summation of the distribution functions in all directions is not constant for each point, although error is less than commonly used lattice Boltzmann method. Fortunately Guo et al [26] proposed one incompressible method, in which, BGK distribution function definition has been changed so that summation of the distribution function, in each point, is constant at all iterations. In the Guo method, which was further simplified by Du et al [31], equilibrium distribution function definition and macroscopic variables relations were changed as follows:

$$s_\alpha(\vec{u}) = w_\alpha[\frac{\vec{e}_\alpha \cdot \vec{u}}{C_S^2} + \frac{(\vec{e}_\alpha \cdot \vec{u})^2}{2C_S^4} - \frac{\vec{u} \cdot \vec{u}}{2C_S^2}] \tag{13}$$

$$f_\alpha^{eq} = \begin{cases} \rho_0 - (1-w_0)\dfrac{P}{C_s^2} + s_0(\vec{u}), \alpha = 0 \\ w_\alpha \dfrac{P}{C_s^2} + s_\alpha(\vec{u}), \alpha = 1 \to 18 \end{cases} \tag{14}$$

In which w_0 and w_α are weight factors which are substituted with Eq. (4), ρ_0 is a fixed quantity such as density of fluid which is a constant value, $C_S = 1/\sqrt{3}$ is speed of sound, P is the fluid pressure and $\vec{u}$ is fluid particle velocity.

$$\rho_0 = \sum_{\alpha=0}^{18} f_\alpha = \sum_{\alpha=0}^{18} f_\alpha^{eq} \tag{15}$$

$$\vec{u} = \sum_{\alpha=1}^{18} \vec{e}_\alpha f_\alpha = \sum_{\alpha=1}^{18} \vec{e}_\alpha f_\alpha^{eq} \tag{16}$$

$$P = \frac{C_s^2}{(1-w_0)}[\sum_{\alpha=1}^{18} f_\alpha + s_0(\vec{u})] = \frac{C_s^2}{(1-w_0)}[\sum_{\alpha=1}^{18} f_\alpha^{eq} + s_0(\vec{u})] \tag{17}$$

By the way, it can be shown that $\sum_{\alpha=0}^{18} w_\alpha = 1$ and $\sum_{\alpha=0}^{18} s_\alpha(\vec{u}) = 0$ thus, in each point, summation of the distribution function for all discretized velocity directions is equal to constant density, independent of its pressure or velocity values.

$$\sum_{\alpha=0}^{18} f_\alpha = \sum_{\alpha=0}^{18} f_\alpha^{eq} = [\rho_0 - (1-w_0)\frac{P}{C_s^2} + s_0(\vec{u})] + \sum_{\alpha=1}^{18}[w_\alpha \frac{P}{C_s^2} + s_\alpha(\vec{u})] = \rho_0 - \frac{P}{C_s^2} + \frac{P}{C_s^2}\sum_{\alpha=0}^{18} w_\alpha + \sum_{\alpha=0}^{18} s_\alpha(\vec{u}) = \rho_0 \tag{18}$$

III. Mass leakage error and mass leakage elimination

In the commonly used lattice Boltzmann method, uniform grid is always used ($dx = dy = dz$) and space step in lattice units is equal to one ($dx = 1$). Therefore, volume around each point (volume of each

element) is equal to one ($V = dxdydz = 1$). By multiplying the volume by the density of that element, mass of that element is achieved ($m = \rho * V$); therefore, the mass of each element is equal to its density ($m = \rho$). On the other hand, each point density is equal to summation of the distribution function in that point, see Eq. (6), thus ($m = \sum_{\alpha} f_{\alpha}$). If this work be done for all points in the domain and results be summed, mass of fluid in the domain is achieved. Therefore mass of fluid is equal to summation of the distribution function in all discrete velocity directions in all points ($fluid\ mass = \sum_{\vec{x}} mass = \sum_{\vec{x}} \sum_{\alpha} f_{\alpha}$). If sum of the distribution function in whole of the domain be changed, total mass of fluid is changed, and change in mass will occur. This mass change is called mass leakage in the literatures [4, 32-34], and can be increasing or decreasing [34]. Since LBGK method is a weakly compressible method, in different iterations, the density in different points is differed and sum of the distribution function in different points is varied, as Eq. (6); therefore, the sum of the distribution function is varied and mass leakage occurs. However, in the Guo incompressible method, summation of the distribution function in each point is kept constant, Eq. (15); therefore mass of fluid in that point and thus in the solution domain, are constant values and there is no mass leakage. Therefore, basic advantage of Guo incompressible method, rather than LBGK or other incompressible methods, is elimination of mass leakage from the simulation. With this advantage, results of Guo method is more accurate than those of the weakly compressible lattice Boltzmann method even for low mach number and low compressibility error.

To illustrate this subject, 2D channel flow around a circular cylinder, and 3D stirred tank fluid flow have been simulated with Guo and LBGK methods. Since LBGK method has been used with low Mach number, compressibility error must be negligible. However, when the above mentioned problems were solved with the two methods, answers were different from each other. Investigations carried out by the author of the present work show that the reason for this different is mass leakage error. Details of the works are presented in the next sections.

IV. Simulated problems

A. *2D channel flow around a cylinder*

For illustration of compressibility and mass leakage effects in the simulation, 2D channel flow around a cylinder, which is a commonly used test case in numerical methods, is considered here [35]. In this work, a cylinder with diameter D=0.1m is placed in a 2D channel with 0.41m*2.2m dimensions. In domain top and down, two stationary walls exist, and for inlet boundary condition parabolic velocity profile, as Eq. (19), is used.

$$u(0, y) = 4u_{\max} y(H - y)/H^2, v = 0 \qquad (19)$$

In which H=0.41m is the channel height and y being the distance from solid wall. Also v is the vertical velocity. Center of cylinder is placed 0.2m distant from down wall and 0.2m distant from inlet of the channel. In this work, density and kinematic viscosity of fluid are considered $1 kg/m^3$ and $10^{-3} m^2/s$, respectively [35]. For the flow in the channel, maximum flow velocity is considered 0.3m/s such that re=20. For application of inlet velocity boundary condition, bounce back boundary condition [36] is used as Eq. (20).

$$f_{\bar{\alpha}} = f_\alpha - 6w_\alpha \vec{e}_\alpha . \vec{u}(0, y) \quad (20)$$

For outlet boundary condition, extrapolation boundary condition is used as Eq. (21). [36]

$$f_\alpha(N_x) = 2 f_\alpha(N_x - 1) - f_\alpha(N_x - 2) \quad (21)$$

In which N_x stands for last index in x direction. And improved Bounce-Back Boundary Condition [37] is used to model the no-slip fluid-solid boundary conditions.

B. Stirred tank fluid flow simulation

In the present work, water flow has been simulated inside a stirred tank with experimental dimensions (10 liter volume) which has four baffles and a six blades Rushton impeller numerically. This geometry is a commonly used geometry in the numerical methods, and there are some numerical and experimental results for it (Fig. 1). The Reynolds number in the stirred tank is defined as $\mathrm{Re} = ND^2/\upsilon$, in which N is the impellers rotational speed (rev/s), D the impeller diameter (m), and υ the kinematic viscosity of working fluid (m^2/s). A Reynolds number of 29000 was chosen for the sake of availability of experimental and numerical data [38]. Since direct numerical simulation of stirred tank flow at industrially relevant Reynolds numbers is not feasible ([1]), large eddy simulation is used in the present study. In a large eddy simulation, resolved scales are solved and small scales are modeled. In this work, a standard smagorinsky model is used for subgrid scale modeling ([20]).

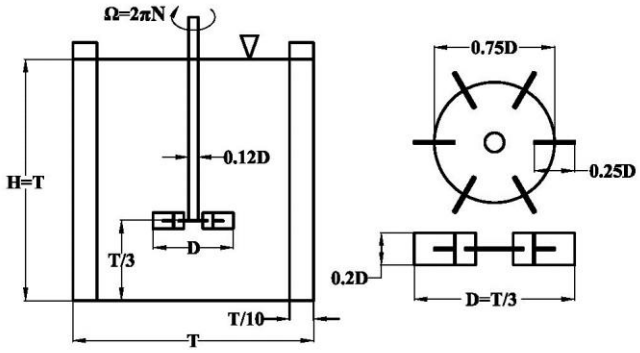

Fig. 1. Flow geometry ([20]), stirred tank (left Fig.) impeller (right Fig.). Disk, blades and baffles thicknesses are 0.017D

By the way, because of turbulent and asymmetry flow in the stirred tank, full 360-degree grids has been simulated. For this purpose, 180^3 square uniform grid, and 19 velocities model have been used. Since this volume of data and its calculations cannot be evaluated with a personal computer, supercomputer and parallel programming were used. In the prepared program, each processor has access to part of data and its numerical grid. In this structure, boundaries data are received/sent from/to neighbor processors. For connection between processors, mpi library functions have been utilized. Fluid flow of the discussed stirred tank has been experimentally investigated in some detail; therefore, results of present work have been compared with previous experimental data. For example, to investigate turbulent flow in stirred tank, total kinetic energy of velocity fluctuations has been calculated from Eq. (22) and compared with experimental results ([38]).

$$k_{tot} = \frac{1}{2}(\overline{u_i u_i} - \bar{u}_i \bar{u}_i) \quad (22)$$

In this Eq., u_i is the i'th velocity component. The averages are over all velocity samples, irrespective of the

angular position of the impeller; and summation convention is used for repeated index i. Velocity fluctuations have been split to two random and periodic parts, and the random part, which has been defined in Eq. (23), has also been compared with available experimental data ([20]).

$$k_{ran}=\frac{1}{2}(\overline{\langle u_i^2\rangle_\theta-\langle u_i\rangle_\theta^2}) \quad (23)$$

In Eq. (23), $\langle\ \rangle_\theta$ is the average value at the angular position θ. And, the over bar denotes averaging over all angular positions. Finally, two overall parameters, power number of stirred tank (N_P) and flow number in exit of blades (N_Q), have been calculated from the results of the two methods. For calculation of power number Eq. (24) has been used

$$N_P=\frac{P}{\rho N^3 D^5} \quad (24)$$

In which P is the power consumed by the blades [39]. And for calculation of flow number Eq. (25) has been used

$$N_Q=\frac{Q_r}{ND^3} \quad (25)$$

In which Q_r is volume flow rate which is exited from blades passages which is computed from Eq. (26).

$$Q_r=2\pi r\int_{z_1}^{z_2}u_r dz \quad (26)$$

In Eq. (26), z_1 and z_2 are the axial positions where the mean radial velocities reached zero [38].

V. Results and discussion

Results of the 2D channel flow simulation are compared to existing numerical and experimental data in table I.

TABLE I. COMPARISON OF FLUID FLOW SIMULATION RESULTS AROUND A CYLINDER

$\mathrm{Re}=20$ $D/dx=80$	**Guo**	**BGK**	**bounds [35]**
C_D	5.5798	5.41	5.57-5.59
C_L	0.01071	0.013	0.0104 0.0110
$\frac{mass(t)-mass(0)}{mass(0)}$ (%)	0.0000034	6.44	-

As seen in this table, results of Guo method are more accurate than LBGK method results, and are lain in permitted bounds. In the present work cylinder diameter was divided to 80 lattice length ([36]) and 330*1762 grid were used. Thus initial mass was 330*1762=581460. If mass leakages which is defined by initial mass minus final mass of fluid domain be recorded, mass leakage of LBGK method becomes equal to 37428 and mass leakage of Guo method is equal to 0.0195, see Fig. 2. Dividing the mass leakages to initial mass, relative mass leakages are 6.44% for LBGK and 0.0000034% for Guo method. It is worth mentioning that LBGK mass leakage, which is deficiency of that method, was increasing during the iterations, while negligible mass leakage in the Guo method, was oscillating around zero and in the author opinion is related to numerical errors. Table I and fig 2 indicate that, for problems which have huge number of iterations and larger grid, elimination of mass leakage is essential, especially when the problem has inlet and/or outlet boundary condition. Small mass leakage is seen when periodic boundary condition is applied to the above mentioned problem for the inlet and outlet boundary conditions [4].

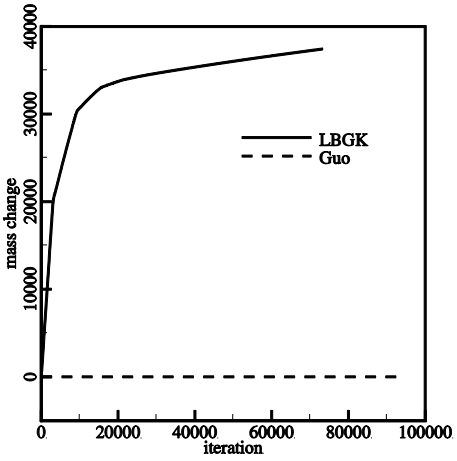

Fig. 2. Mass leakage in simulation of 2D channel flow around a cylinder

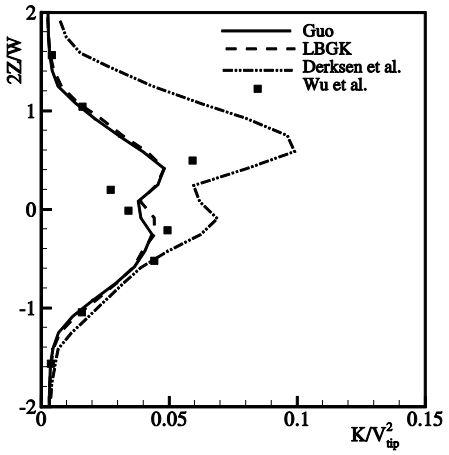

Fig. 3. Comparison of random part of turbulent kinetic energy, $2r/D=1.07$, Guo incompressible LBM (Guo), weakly compressible LBM (LBGK), Derksen et al. numerical simulation([20]) and Wu et al. experiment ([38]).

To better understand the effect of compressibility and mass leakage error, fluid flow has been simulated numerically in a stirred tank at the present work. In Figs. 3 and 4, random and total parts of turbulent kinetic energy of the stirred tank flow have been compared with numerical ([20]) and experimental ([38]) data.

As is seen in these Figs, the results of the present work predict the behavior of kinetic energy of turbulence very well, and with respect to previous numerical simulation ([20]), these results are more compatible to the experimental results. However, comparing Guo and LBGK results, little difference is seen. The reason for the little difference is a little mass leakage in this simulation.

If mass leakage be investigated in this stirred tank (Fig 5), it will be seen that the mass leakage is nearly zero for Guo method and is equal to 83881 in LBGK method. Dividing to 180^3, relative mass leakage is nearly zero for Guo and 1.4% for LBGK methods. Thus mass leakage effect is negligible in each point of interior domain.

Due to availability of experimental data [20] for phase averaged velocity, in the vicinity of moving blades, their values prepared with the two methods and with the experimental data have been shown in Fig 6. As is seen in that Fig., the present work's numerical simulation is in good agreement with the experimental results. However, with little attention, it can be seen that the results of Guo method are more matched to experimental results. For this purpose, as an example, top row of velocity vectors can be seen in Fig. 6.

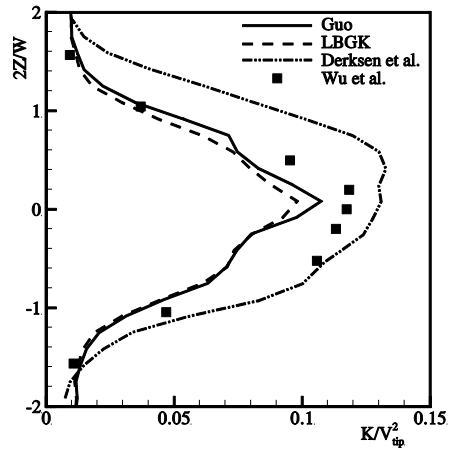

Fig. 4. Comparison of total turbulent kinetic energy, $2r/D=1.07$, Guo incompressible LBM (Guo), weakly compressible LBM (LBGK), Derksen et al. numerical simulation([20]) and Wu et al. experiment ([38]).

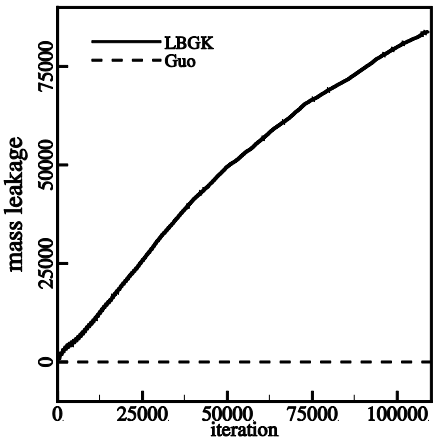

Fig. 5. Mass leakage in stirred tank flow simulation with LBGK and Guo methods

In this Fig., from experimental results, it can be seen that the fluid in top row was deviated to top and this can be seen in Guo results clearly but in LBGK results, it cannot be seen or it can be seen with difficulty. As was said before, due to small mass leakage in this simulation, (approximately 1.4%), the difference in results of the two methods is small in each point. To better understand the benefits of Guo method rather than LBGK method, two overall parameters, power number of stirred tank (N_P) and flow number in exit of blades (N_Q), have been calculated. Power number of 5.7 has been reported for Re=29000 by Derksen and Van Den Aker [20]. However, in [39] and [40], it has been said that the power number depends on blade thickness in addition to Reynolds number, and for Re=29000 and the blade thickness of 0.017D, which had been used in [20] and present study, power number of 5.2 has been reported in a chart approximately. Results of present work have been presented in table II, and it can be seen that the results of Guo method is closer to experimental data. This is also true in the case of flow number. Fig. 7 has been prepared to show flow number variation and compares present study results with some other works. Results of present study are approximately in middle of other works results. Also Guo and LBGK results are near to each other locally. But table II shows that with respect to LBGK results, Guo results are closer to experimental data.

Consequently, it can be deduced that because of small mass change in each point, local flow quantities are the same in the two methods. However, due to accumulation of mass change in whole of the domain, overall flow quantities are different because of different mass leakage in the two methods.

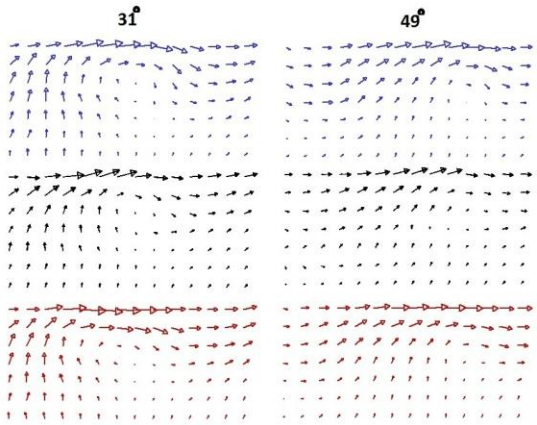

Fig. 6. Phase averaged velocity field in vicinity of impeller, in two degrees with respect to an impeller blade. Guo method (top row), experimental data (middle row) ([20]), and LBGK method (down row)

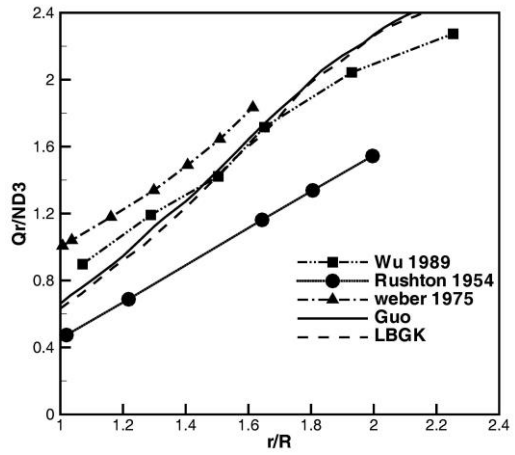

Fig. 7. Flow number in exit of blades. Results of present study and some other works as reported in [38]

TABLE II. COMPARISON OF SOME OVERALL PARAMETERS, POWER AND FLOW NUMBERS, IN TWO SIMULATIONS AND EXPERIMENTAL DATA IN A STIRRED TANK

quantity	**LBGK**	**Guo**	**Experiment**
Power number (N_P)	4.95	5.32	5.2 [39]
Flow number (N_Q)	0.66	0.6	0.73 [41]
	0	9	
$\frac{mass(t)-mass(0)}{mass(0)}$ (%)	1.4	0.0	-

VI. Conclusions

In this paper, weakly compressible lattice Boltzmann method and Guo incompressible lattice Boltzmann method have been compared. It has been shown that Guo incompressible method eliminates not only the compressibility error, but also the mass leakage error from the weakly compressible lattice Boltzmann method. Also, it has been shown that because of small mass leakage error in each point, the results of incompressible Guo method for the local flow quantities are similar to those of weakly compressible lattice Boltzmann method. However, because of accumulation of mass leakage error in whole of the domain, results of Guo incompressible method are more accurate than those of weakly compressible method for overall flow quantities. It can be seen in table II that mass leakage error in LBGK method is about 1.4% while it is about 0% in Guo method. Therefore Guo method results are more accurate than LBGK results.

VII. Nomenclatures

Velocity in lattice Boltzmann	c
Drag coefficient (dimensionless)	C_D
Lift coefficient (dimensionless)	C_L
Impeller diameter (m)	D
Velocity Direction in LBM	e
Distribution function, fluid point	f
Index of velocity direction	i
Kinetic energy of turbulence	k
Angular velocity (rev/s)	N

Power number (dimensionless)	N_p
Flow number (dimensionless)	N_Q
Reynolds number	Re
Time (s)	t
Velocity component (m/s)	u
Weight factor, wall location/velocity index	w
Coordinate location (m)	x
Index of distribution function	α
Kinematic viscosity (m^2/s)	ν
Relaxation time (s)	λ
Density (kg/m^3)	ρ, ρ_0
Angular coordinate location (rad)	θ
Dimension less relaxation time	τ

References

[1] Eggels, J. G. M., "Direct and large-eddy simulation of turbulent fluid flow using the lattice-boltzmann scheme," *International journal of heat and fluid flow*, vol. 17, pp. 307-323, 1996.

[2] Musavi, S. H. and Ashrafizaadeh, M., "On the simulation of porous media flow using a new meshless lattice boltzmann method," in *Mathematical and computational approaches in advancing modern science and engineering*: Springer, pp. 469-480, 2016.

[3] Musavi, S. H. and Ashrafizaadeh, M., "A mesh-free lattice boltzmann solver for flows in complex geometries," *International journal of heat and fluid flow*, vol. 59, pp. 10-19, 2016.

[4] Oulaid, O. and Zhang, J., "On the origin of numerical errors in the bounce-back boundary treatment of the lattice boltzmann method: A remedy for artificial boundary slip and mass leakage," *European Journal of Mechanics-B/Fluids*, vol. 53, pp. 11-23, 2015.

[5] Musavi, S. H. and Ashrafizaadeh, M., "Meshless lattice boltzmann method for the simulation of fluid flows," *Physical Review E*, vol. 91, p. 023310, 2015.

[6] Khazaeli, R., Mortazavi, S., and Ashrafizaadeh, M., "Application of an immersed boundary treatment in simulation of natural convection problems with complex geometry via the lattice boltzmann method," *Journal of Applied Fluid Mechanics*, vol. 8, pp. 309-321, 2015.

[7] Khazaeli, R., Ashrafizaadeh, M., and Mortazavi, S., "A ghost fluid approach for thermal lattice boltzmann method in dealing with heat flux boundary condition in thermal problems with complex geometries," *Journal of Applied Fluid Mechanics*, vol. 8, pp. 439-452, 2015.

[8] Zadehgol, A., Ashrafizaadeh, M., and Musavi, S. H., "A nodal discontinuous galerkin lattice boltzmann method for fluid flow problems," *Computers & Fluids*, vol. 105, pp. 58-65, 2014.

[9] Zadehgol, A. and Ashrafizaadeh, M., "Introducing a new kinetic model which admits an h-theorem for simulating the nearly incompressible fluid flows," *Journal of Computational Physics*, vol. 274, pp. 803-825, 2014.

[10] Xiong, Q., Madadi-Kandjani, E., and Lorenzini, G., "A lbm dem solver for fast discrete particle simulation of particle fluid flows," *Continuum Mechanics and Thermodynamics*, vol. 26, pp. 907-917, 2014.

[11] Walther, E., Bennacer, R., and Desa, C., "Lattice boltzmann method applied to diffusion in restructured heterogeneous media," *Defect and Diffusion Forum*, pp. 237-242, 2014.

[12] Viggen, E. M., "The lattice boltzmann method: Fundamentals and acoustics," 2014.

[13] Rahmati, A. R. and Niazi, S., "Entropic lattice boltzmann method for microflow simulation," *Nanomechanics Science and Technology: An International Journal*, vol. 5, 2014.

[14] Rahmani, G. M. and Ashrafizaadeh, M., "Simulation of pressurization step of a psa process using the multi-component lattice boltzmann method," 2014.

[15] Naghavi, S. M. and Ashrafizaadeh, M., "A comparison of two boundary conditions for the fluid flow simulation in a stirred tank," *JCME*, vol. 33, pp. 15-30, 2014.

[16] Zhuo, C., Zhong, C., Guo, X., and Cao, J., "Mrt-lbm simulation of four-lid-driven cavity flow bifurcation," *Procedia Engineering*, vol. 61, pp. 100-107, 2013.

[17] Yang, F. L., Zhou, S. J., Zhang, C. X., and Wang, G. C., "Mixing of initially stratified miscible fluids in an eccentric stirred tank: Detached eddy simulation and volume of fluid study," *Korean Journal of Chemical Engineering*, vol. 30, pp. 1843-1854, 2013.

[18] Wang, L., Zhang, B., Wang, X., Ge, W., and Li, J., "Lattice boltzmann based discrete simulation for gasâ€“solid fluidization," *Chemical engineering science*, vol. 101, pp. 228-239, 2013.

[19] Wang, L., Zhang, B., Wang, X., Ge, W., and Li, J., "Lattice boltzmann based discrete simulation for gas-solid fluidization," *Chemical engineering science*, vol. 101, pp. 228-239, 2013.

[20] Derksen, J. and Van den Akker, H. E. A., "Large eddy simulations on the flow driven by a rushton turbine," *AIChE Journal*, vol. 45, pp. 209-221, 1999.

[21] Guha, D., Ramachandran, P. A., Dudukovic, M. P., and Derksen, J. J., "Evaluation of large eddy simulation and euler-euler cfd models for solids flow dynamics in a stirred tank reactor," *AIChE Journal*, vol. 54, pp. 766-778, 2008.

[22] Derksen, J. J., "Solid particle mobility in agitated bingham liquids," *Industrial & Engineering Chemistry Research*, vol. 48, pp. 2266-2274, 2009.

[23] Derksen, J. J., "Agitation and mobilization of thixotropic liquids," *AIChE Journal*, vol. 56, pp. 2236-2247, 2010.

[24] Derksen, J. J., "Direct flow simulations of thixotropic liquids in agitated tanks," *The Canadian Journal of Chemical Engineering*, vol. 89, pp. 628-635, 2011.

[25] Derksen, J. J., "Simulations of mobilization of bingham layers in a turbulently agitated tank," *Journal of Non-Newtonian Fluid Mechanics*, vol. 191, pp. 25-34, 2013.

[26] Guo, Z., Shi, B., and Wang, N., "Lattice bgk model for incompressible navier-stokes equation," *Journal of Computational Physics*, vol. 165, pp. 288-306, 2000.

[27] Yu, D., Mei, R., Luo, L. S., and Shyy, W., "Viscous flow computations with the method of lattice boltzmann equation," *Progress in Aerospace Sciences*, vol. 39, pp. 329-367, 2003.

[28] Du, R. and Liu, W., "A new multiple-relaxation-time lattice boltzmann method for natural convection,"

Journal of Scientific Computing, vol. 56, pp. 122-130, 2013.

[29] He, X. and Luo, L. S., "Lattice boltzmann model for the incompressible navier stokes equation," *Journal of Statistical Physics,* vol. 88, pp. 927-944, 1997.

[30] Dellar, P. J., "Incompressible limits of lattice boltzmann equations using multiple relaxation times," *Journal of Computational Physics,* vol. 190, pp. 351-370, 2003.

[31] Du, R., Shi, B., and Chen, X., "Multi-relaxation-time lattice boltzmann model for incompressible flow," *Physics Letters A,* vol. 359, pp. 564-572, 2006.

[32] Bao, J., Yuan, P., and Schaefer, L., "A mass conserving boundary condition for the lattice boltzmann equation method," *Journal of Computational Physics,* vol. 227, pp. 8472-8487, 2008.

[33] Chun, B. and Ladd, A. J. C., "Interpolated boundary condition for lattice boltzmann simulations of flows in narrow gaps," *Physical Review E,* vol. 75, p. 66705, 2007.

[34] Krüger, T., Varnik, F., and Raabe, D., "Shear stress in lattice boltzmann simulations," *Physical Review E,* vol. 79, p. 46704, 2009.

[35] Schaefer, M., Turek, S., Durst, F., Krause, E., and Rannacher, R., "Benchmark computations of laminar flow around a cylinder," *Notes on numerical fluid mechanics,* vol. 52, pp. 547-566, 1996.

[36] Peng, Y. and Luo, L. S., "A comparative study of immersed-boundary and interpolated bounce-back methods in lbe," *Progress in Computational Fluid Dynamics, an International Journal,* vol. 8, pp. 156-167, 2008.

[37] Mei, R., Yu, D., Shyy, W., and Luo, L. S., "Force evaluation in the lattice boltzmann method involving curved geometry," *Physical Review E,* vol. 65, p. 041203, 2002.

[38] Wu, H. and Patterson, G. K., "Laser doppler measurements of turbulent flow parameters in a stirred mixer," *Chemical engineering science,* vol. 44, pp. 2207-2221, 1989.

[39] Chapple, D., Kresta, S. M., Wall, A., and Afacan, A., "The effect of impeller and tank geometry on power number for a pitched blade turbine," *Trans ICheme,* vol. 80, pp. 364-372, 2002.

[40] Rutherford, K., Mahmoudi, S. M. S., Lee, K. C., and Yianneskis, M., "The influence of rushton impeller blade and disk thickness on the mixing characteristics of stirred vessels," *Trans ICheme,* vol. 74, pp. 369-378, 1996.

[41] Costes, J. and Couderc, J. P., "Study by laser doppler anemometry of the turbulent flow induced by a rushton turbine in a stirred tank: Influence of the size of the units i. Mean flow and turbulence," *Chemical engineering science,* vol. 43, pp. 2751-2764, 1988.